Iraqi Journal of Science

ISSN: 0067-2904

Signature of Plasmonic Nanostructures Synthesised by Electrical Exploding Wire Technique on Surface-Enhanced Raman Scattering

Fouad G. Hamzah*, Hammad R. Humud
Department of Physics, College of Science, University of Baghdad, Baghdad, Iraq

Received: 1/3/2020 Accepted: 9/8/2020

Abstract

This work aims to fabricate two types of plasmonic nanostructures by electrical exploding wire (EEW) technique and study the effects of the different morphologies of these nanostructures on the absorption spectra and Surface-Enhanced Raman Scattering (SERS) activities, using Rhodamine 6G as a probe molecule. The structural properties of these nanostructures were examined using X-Ray diffraction (XRD). The morphological properties were examined using field emission scanning electron microscopy (FESEM) and scanning transmission electron microscopy (STEM). The absorption spectra of the mixed R6G laser dye (concentration 1×10^{-6} M) with prepared nanostructures were examined by double beam UV-Vis Spectrophotometer. The Raman spectra of the R6G mixed with the prepared nanostructures were examined using a Horiba HR Evolution 800 Raman microscope system with an objective lens (50 ×). The FESEM and STEM images indicated that the Ag nanoparticles (AgNPs) with 35 nm average particle sizes were decorated on the surface of the AgNWs and the PDA layer by EEW technique, forming AgNW@AgNPs and AgNW@PDA@AgNPs nanostructures. The results indicated that the increased intensities of the absorption spectra peaks and the SERS arise from the hot spots and the roughness of the surface of nanostructures. The SERS enhancement factor of R6G (1×10^{-6} M) was reached at 2.3×10^{7} and 2.5×10^{7}, at the wave number of 1650 cm^{-1}, for the AgNW@AgNPs and AgNW@PDA@AgNPs nanostructures, respectively, after being excited by ($\lambda_{exc.}$ = 532 nm) laser source. It can be concluded that the AgNW@AgNPs and AgNW@PDA@AgNPs nanostructures were fabricated with an easy and simple way without the need for additional chemical compounds. These nanostructures attained a reliable and sensitive detection and can be utilized in a variety of SERS applications, such as chemical and biological sensors.

Keywords: Surface-Enhanced Raman Scattering (SERS), Electrical exploding wire, Surface plasmon resonance, Enhancement factor, R6G dye.

بصمة التراكيب النانوية البلازمونية المتولدة بتقنية التفجير الكهربائي للسك على تشتت رامان المحسن السطح

فؤاد جعيله حمزة *, حمد رحيم حمود
قسم الفيزياء، كلية العلوم، جامعة بغداد، بغداد، العراق

الخلاصة

يهدف هذا العمل إلى تصنيع نوعين من التراكيب النانوية البلازمية بتقنية سلك التفجير الكهربائي (EEW) ودراسة تأثير المورفولوجيا المختلفة لهذه التراكيب النانوية البلازمية على أطياف الامتصاص وعلى

*Email: fghhamzah@gmail.com

أنشطة تشتت رامان المحسنة السطح (SERS) باستخدام صبغة R6G كجزيئة مجس. لقد تم فحص الخصائص التركيبية لهذه التراكيب النانوية باستخدام حيود الأشعة السينية (XRD). وقد تم فحص المورفولوجية باستخدام Field emission scanning electron microscope (FESEM) و scanning transmission electron microscopy (STEM) وتم فحص أطياف الامتصاص للصبغة الليزرية R6G (بتركيز 1×10^{-6} M) قبل وبعدما مزجت مع التراكيب النانوية المحضرة بواسطة double beam UV–Vis Spectrophotometer. وكذلك تم فحص أطياف رامان لصبغة R6G الممزوجة مع التراكيب النانوية المحضرة باستخدام نظام رامان Horiba HR Evolution 800 ذي عدسة شيئية ذات تكبير (× 50). لقد اظهرت نتائج صور FESEM وSTEM إلى أن متوسط حجم جسيمات الفضة النانوية بلغ فيها 35 nm قد تم تزيينها على سطح AgNWs وطبقة PDA بواسطة تقنية EEW لتشكيل التراكيب النانوية (AgNW@AgNPs) و (AgNW@PDA@AgNPs). أشارت النتائج إلى أن الشدة المتزايدة لقمم أطياف الامتصاص وSERS تنشأ من النقاط الساخنة وخشونة سطح التراكيب النانوية، حيث بلغ عامل التحسين لطيف رامان لصبغة R6G (بتركيز 1×10^{-6} M) الى (2.3×10^{7}) و (2.5×10^{7}) عند العدد الموجي ($1650\ cm^{-1}$) للتراكيب النانوية (AgNW@AgNPs) و (AgNW@PDA@AgNPs) على الترتيب، بعد أن تم اثارتها بالمصدر الليزري ذي الطول الموجي ($\lambda_{exc.}$ = 532 nm). يمكن أن نستنتج أن التراكيب النانوية البلازمونية (AgNW@AgNPs) و (AgNW@PDA@AgNPs) قد تم تصنيعها بطريقة سهلة وبسيطة دون استخدام أي من المركبات الكيميائية. لقد حصلت الهياكل النانوية (AgNW@AgNPs) و (AgNW@PDA@AgNPs) على كشف موثوق وحساس، لذا يمكن استخدامها في مجموعة متنوعة من تطبيقات SERS مثل المستشعرات الكيميائية والبيولوجية.

Introduction

Recently, fabrication of nanomaterials using physical techniques, especially those created using electro-exploding wire (EEW) technique has received remarkable consideration because of its high purity (no requirement for additives as those used in the chemical means) and fast preparation. In addition, the resulting nanoparticles retain the chemical identity of the original materials and are therefore capable of producing metal nanomaterials for any required chemical [1]. Nanoparticles can be synthesized through the EEW technique, while surrounded by a non-flammable liquid medium, such as deionized water. The particles evaporated during the explosion will condense into the liquid more efficiently than into the surrounding air. The properties of nanoparticles created by EEW rely upon numerous parameters, which include wires' material and diameter, features of the electrical circuit, and the surrounding medium [2].

Noble metal nanostructures show unique optical properties because of the excitation of localized plasmons [3], which have been widely used to control a variety of optical signals [4]. The optical properties enhancement, especially Surface Enhanced Raman Scattering (SERS), using metal nanostructures is considered one of the most efficient methods for ultra-sensitive chemical sensing of molecules adsorbed on the surface of metal nanostructure substrates. The active SERS substrates provide a large enhancement to Raman signals, which can be mainly attributed to two mechanisms; the first is the chemical mechanism based on the transfer of charge between molecules and metallic substrates. The second is the electromagnetic mechanism, which is based on the enhancement of local electromagnetic fields because of the resonance of surface plasmons stimulated by incident light [5]. The enhancement of large electromagnetic fields occurs in active positions (hot spots) on the metal's surface at a nanometre gap between two nanoparticles, due to coupling the Localized Surface Plasmon Resonance (LSPR) between them [6]. Therefore, it has been necessary to fabricate nanostructures, containing rough surface and having a large number of hot spots, which serve as effective substrates to enhance Raman spectrum. Therefore, a high density of AgNPs on the surface of AgNWs and the AgNW@PDA which served as SERS hot spots was designed and fabricated for increasing SERS intensity and target molecule detection (R6G dye molecules). As it is well known, the influence of hot spots depends on the size and shape of the nanoparticles and the space between two neighboring nanoparticles. Theoretical calculations showed that the spacing of neighboring nanoparticles on any surface can provide a strongly enhanced Raman signal, with the likelihood of having greatest enhancement of SERS in the presence of nanogaps between the metal nanostructures [7]. Several

pioneering works verify that strong SERS intensity should occur when the wavelength of LSPR overlaps with the excitation laser wavelength [8]. Therefore, development of reliable as well as low-cost and simple preparation techniques of the noble metal nanostructures, which contain rough surfaces and active hot spot, are our priorities in this research.

At the present time, the noble metallic nanomaterials, such as gold, silver, and copper are widely used in the manufacture of active SERS substrates, due to noble metal nanoparticles that could generate a powerful local electric field with the excitation of incident light [9]. Compared to other noble metal nanomaterials, silver nanostructures are more widely utilized as an active SERS substrate through exploiting their wide range of plasmon resonance influences in the visible region, strong signal enhancement, and reliable synthesis technique [10]. So far, silver nanostructures with varied morphologies, such as nanospheres [11], nanorods [12], nanowires [13], and nanosheets [14], have been described as active SERS substrates that attain very sensitive molecular detection. Among the nanostructures mentioned above, the metal nanostructures with rougher surfaces (e.g. AgNPs decorated AgNWs forming metal-metal nanostructures) are utilized as active SERS structures in scientific researches or highly sensitive application fields [15]. These nanostructures allow increasing the electric fields resulting from the LSPR of AgNPs and their overlap with those from the SPR of AgNWs. Thus, they achieve high intensity for SERS [16].

Dopamine (DA) has plentiful catechol and amine active groups that exist on the surface of molecules. These groups could be employed as a multipurpose rostrum due to their distinguished properties, for example, anchor ability, chemical recognition, and self-polymerization [17]. Especially, the self-polymerization of DA could supply a facilitated and effective method to surface adjustment and create a very strong adhesive layer by immersing the material into the solution. More importantly, due to the existence of plenty of groups from catechol and amine on the surface, polydopamine (PDA) molecules could have fairly robust complexing behaviours with metallic ions, and they can automatically in situ reduce them into the metallic nanoparticles via oxidizing catechol into the correspondent quinine groups under alkaline aqueous solution [18].

At the present time, regular metal nanostructures with desired size and coating are deposited on all types of substrates, even including super hydrophobic surface, which supplied a promising opportunity to create sharp edges and nanogaps as controllable SERS "hot spots" on the AgNWs surface. Therefore, from these unique properties of PDA, an effective and multipurpose strategy was developed to controllably synthesize a series of AgNW@PDA@AgNPs nanostructures based on AgNWs that are coated with PDA molecules, which achieved highly a sensitive detection to SERS. By EEW technique, the AgNPs were decorated on the surface of PDA layer for the formation of metal-insulator-metal nanostructures, which allow increasing the electric fields resulting from the LSPR of AgNPs and their overlap with those from the SPR of AgNWs. For the nanostructure of AgNW@PDA@AgNPs, there were the two types of coupling localized surface plasmon- localized surface plasmon (LSP-LSP) and control localized surface plasmon-surface plasmon polariton (LSP-SPP) by PDA layer. The AgNW@PDA@AgNPs nanostructures could give a large number of "hot spots" and showed ultra-high sensitivity of SERS by the regulation of a synergistic effect between the AgNWs and AgNPs along the longitudinal axis. It could be possible by this fabrication strategy to demonstrate a large capability to fabricate varied-active substrates and attain reliable and sensitive detection in chemical and biological fields.

Experimental Section

1- *Materials and characterization instruments*

Rhodamine 6G (R6G) ($C_{28}H_{31}N_2O_3Cl$, molecular weight 479.02 g/Mol) was purchased from Exciton Chemical CO.INC. The dye solution was prepared by gravimetric method, where 0.47902 g of the dye powder was dissolved in 10 ml of deionized water to produce a solution of the R6G dye with a concentration of 1×10^{-1} M. Then, by the dilution method, we obtained dye concentrations from 1×10^{-1} to 1×10^{-6} M). Silver nanowire (AgNW) was purchased from XFNANO with an average diameter of 90 nm and length of 1 micron. A weight of 500 mg was dissolved in 25 ml water, reaching a concentration of ≈ 0.2 M. Dopamine hydrochloride (tris-base, ≥ 99.9 %) was purchased from Sigma-Aldrich. Silver wire with a diameter of 0.3 mm and silver plate (3cm x 2cm x 3mm) at 99.9% purity were purchased from a jeweller shop in Baghdad-Iraq. Raman spectra of the prepared samples were recorded using a Horiba HR Evolution 800 Raman microscope system, after being excited with a 532 nm laser (objective lens 50 ×). The integration time was 8 seconds and the laser power was 1 mW.

Raman spectra of the R6G dye were measured for different concentrations after mixing it with the plasmonic nanostructures. These samples were examined after placing few drops of the mixture on a glass substrate and drying them under ambient condition. The absorption spectra of the mixed R6G with the prepared nanostructures were measured in different concentrations in the wavelength range of 300-800 nm at room temperature for all samples, using Shimadzu-1800 UV-VIS double beam spectrophotometer. The concentration of AgNPs prepared by EEW technique was measured using AA-7000 Atomic Absorption Spectrophotometer (Shimadzu). The details of internal nanostructure features were examined by XRD; few drops of the aqueous colloid of AgNPs, AgNWs, AgNW@AgNPs, AgNW@PDA and AgNW@PDA@AgNPs nanostructures were dried on glass substrate and XRD data were taken in the range of 2θ (10–90) degree. The XRD was performed with XRD 6000 X-ray Diffractometer (Shimadzu) using $CuK\alpha_1$ with radiation of λ= 1. 5406 Å. The morphologies of the AgNWs and AgNW@AgNPs nanostructures were characterized with a field-emission scanning electron microscope. The analysis was performed on samples deposited onto a rinsed silicon wafer and dried under ambient conditions. The particles size and morphologies of AgNPs, AgNW@PDA, and AgNW@PDA@AgNPs nanostructures were further characterized by STEM (FESEM, STEM Nova NanoSEM 450) with 1000 KV accelerating voltage.

2- *Preparation of nanostructures*

2.1- *Preparation of AgNPs by EEW technique*

A volume of 30 ml of deionized water was placed in a shock wave resistant container with magnetic stirring for the entire time of preparation at room temperature, as shown in Figure-1. Preparation of AgNPs was achieved by exploding a highly pure Ag wire (0.3 mm in diameter) against an Ag plate that was held under a voltage of 82.2 V respect to the wire and a steady current of 100A . The electric exploding of the wire was performed by touching the wire with the plate mechanically. The concentration of the prepared AgNPs was 2×10^{-4} M, which was diluted to obtain other concentrations.

2.2- *Preparation of AgNW@AgNPs nanostructures*

To prepare the AgNWs decorated by AgNPs, 1.25 ml of aqueous colloid of the AgNWs (0.2 M) was dispersed by 30 ml deionized water. For the purpose of obtaining a homogeneous aqueous colloid, magnetic stirrer was used for 30 min at room temperature, followed by ultra-sonication for 15 min to ensure complete dispersion. The final aqueous colloid of AgNWs was placed in shock wave resistant container. Then, the same steps were used for forming AgNW@AgNPs nanostructures (e.g. metal-metal nanostructures).

2.3- *Preparation of AgNW@PDA@AgNPs nanostructures*

A volume of 1.25 ml of aqueous colloid of the AgNWs (0.2 M) was dispersed in 30 ml deionized water with magnetic stirring for 30 min at room temperature, then ultra-sonicated for 15 min for the purpose of ensuring complete dispersion. Then, 0.05 g of dopamine hydrochloride powder was added into the aqueous colloid of the AgNWs. The pH of the final reaction solution was adjusted to 8.5 by adding Tris-HCl buffer solution with a gentle stirring speed at room temperature for 24 hours. When the color of the aqueous colloid was started to become brown, this was an indication that the polydopamine has coated the AgNWs. After centrifuging the solution at 4000 rpm and washing with deionized water several times, the AgNWs@PDA were obtained and stored in deionized water to be used later. Then, the PDA-coated AgNWs were dispersed in 30 ml deionized water with ultrasonicating. The final aqueous colloid of the AgNWs@PDA was decorated by AgNPs using the EEW technique for forming AgNW@PDA@AgNPs nanostructures (e.g. metal-insulator-metal-nanostructures).

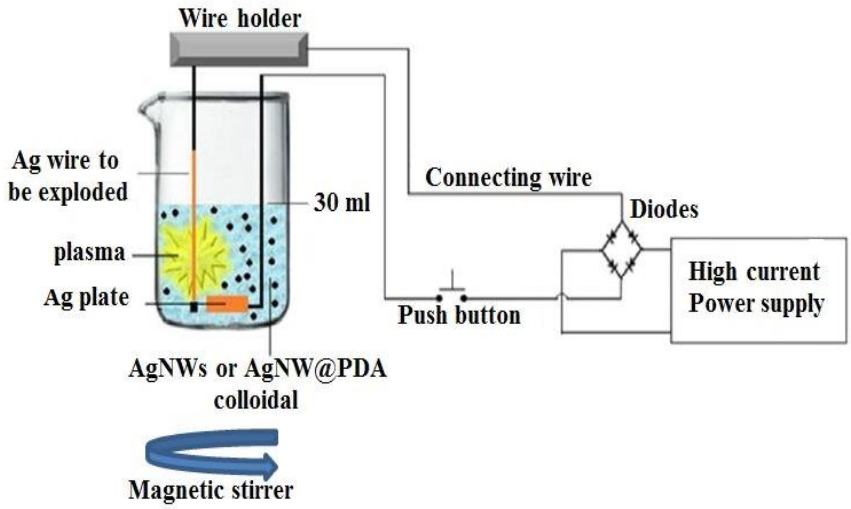

Figure 1-Experimental set-up for fabricating AgNPs, AgNW@AgNPs and AgNW@PDA@AgNPs nanostructures.

2.4- *Preparation of SERS substrates*

The R6G (1×10^{-6} M) dye was mixed with AgNW@AgNPs and AgNW@PDA@AgNPs nanostructures, respectively, then deposited on glass substrates and allowed to dry under the ambient conditions before examining the Raman spectrum, as illustrated in Figure-2.

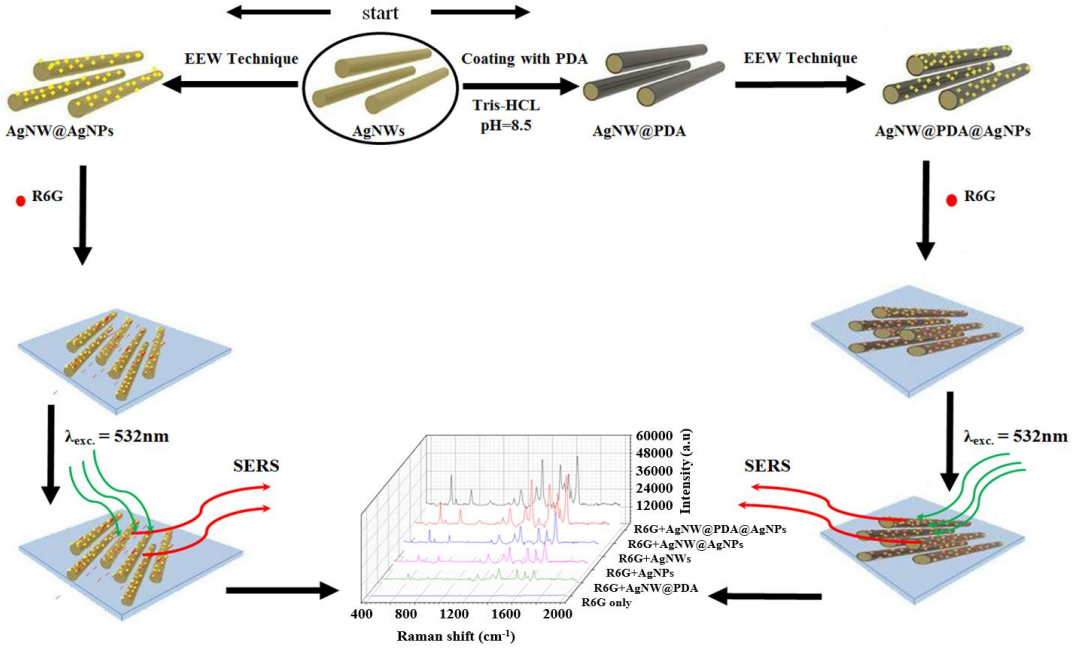

Figure 2-Schematic representation for the construction of AgNW@PDA@AgNPs and AgNW@AgNPs nanostructures and using them in the examination of SERS.

Results and discussion

1- *X-ray Diffraction Patterns of AgNPs, AgNWs, AgNW@AgNPs, AgNW@PDA and AgNW@PDA@AgNPs nanostructures.*

Figure-3 shows typical XRD patterns of AgNPs, AgNWs, AgNW@AgNPs, AgNW@PDA and AgNW@PDA@AgNPs nanostructures. The results demonstrated that the prepared AgNPs, AgNW@AgNPs and AgNWs@PDA@AgNPs nanostructures are having face-centred cubic phase for

Ag metal. All patterns have five peaks with a slight difference in the peak location of each sample, which were observed at (2θ) degrees of 38.116 °, 44.227 °, 64.425 °, 77.472 ° and 81.536 ° and have been indexed to hkl values of (111), (200), (220), (311) and (222), respectively. This indicates that no oxidation occurred during and after the preparation of AgNPs, AgNW@AgNPs and AgNW@PDA@AgNPs nanostructures by EEW technique and that the high purity and good crystalline nature were preserved. The peak position of the XRD pattern is similar to that of the standard bulk silver, which corresponded with the face-centred cubic structure of silver metal (identical with JCPDS Card No. 4-0783).

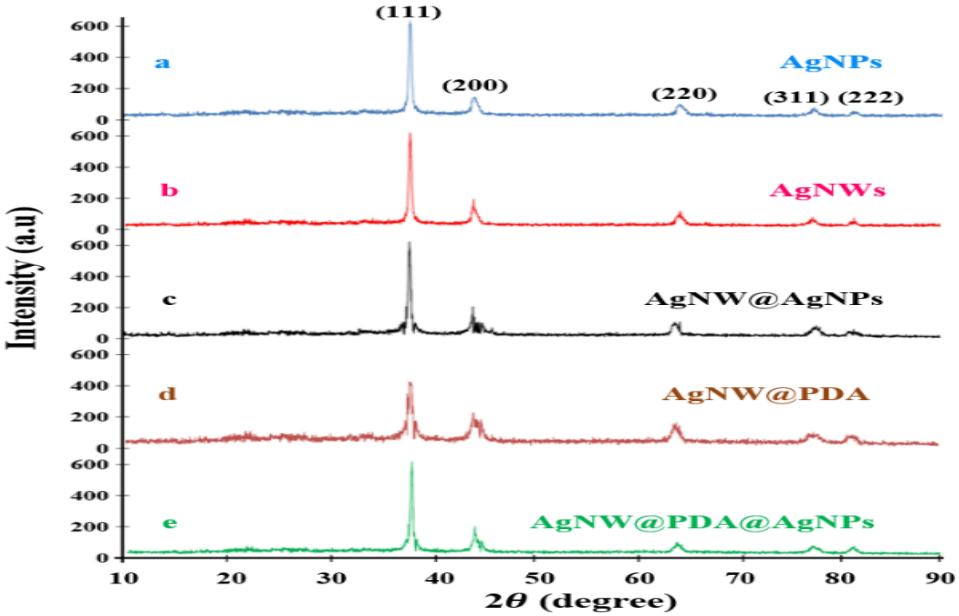

Figure 3-X-ray Diffraction Patterns of (a) AgNPs (b) AgNWs (c) AgNW@AgNPs (d) AgNW@PDA and (e) AgNW@PDA@AgNPs nanostructures.

2- ***STEM image analyses***

Figure-4 demonstrates the morphology, structural information, and particle size of the AgNPs, AgNW@PDA and AgNW@PDA@AgNPs. As shows in Figure- 4a, the average size of AgNPs was 35nm. The AgNPs were nearly spherical and slightly agglomerated. As clearly observed in Figure- 4b, the PDA layer could be fixed onto AgNWs surface and the AgNWs was coated completely to form the AgNW@PDA nanostructure, where the AgNWs acted as the core and PDA formed the amorphous shell. Figure- 4b demonstrates that the DA molecules coated the surface of AgNWs, with the creation of assembled functional PDA layer by self-polymerization. Figure- 4c shows that the density and the distribution of AgNPs decorated on AgNW@PDA surface were random. The AgNPs were adhered to the AgNW@PDA surface very tightly to form the AgNW@PDA@AgNPs nanostructures. The PDA layer served as a spacer molecule (nanogap) to separate the two metals (AgNWs and AgNPs). The density of the AgNPs on the surface of the AgNW@PDA nanostructures depended on the number of explosions. The distance between the two the nanostructures was in the magnitude of several nanometers, which is the ideal distance for the existence of effective hot spots due to electromagnetic coupling, which depends on PDA thickness [11,19].

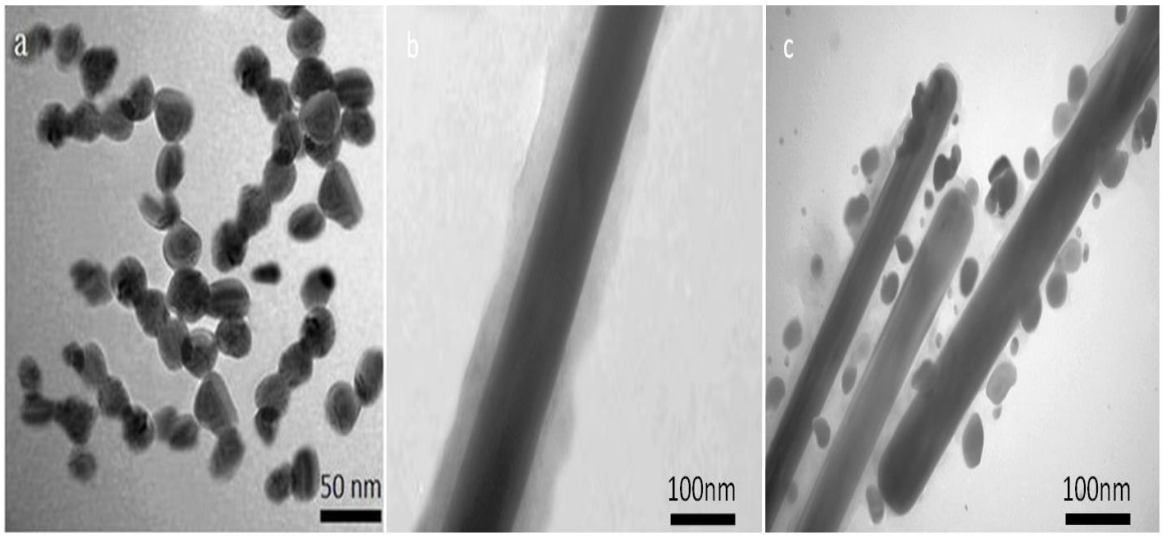

Figure 4-STEM images of (a) AgNPs, (b) AgNW@PDA and (c) AgNW@PDA@AgNPs.

3- ***FESEM image analyses***

Figure- 5a illustrates that the AgNWs have a uniform straight morphology and smooth surface. In Figure-5b, the AgNW@AgNPs nanostructures displayed a relatively irregular morphology, which indicates that AgNWs surface was decorated by AgNPs. After performing the EEW technique, many silver nanoparticles appeared on the surface of AgNWs along the long axis, and all of the AgNWs were successfully decorated with AgNPs and formed a series of AgNW@AgNPs nanostructures. Also, it can be seen that the scattered AgNPs were adhered tightly and randomly to the AgNWs surface, forming an irregular rough surface that contains plentiful hot spots [20].

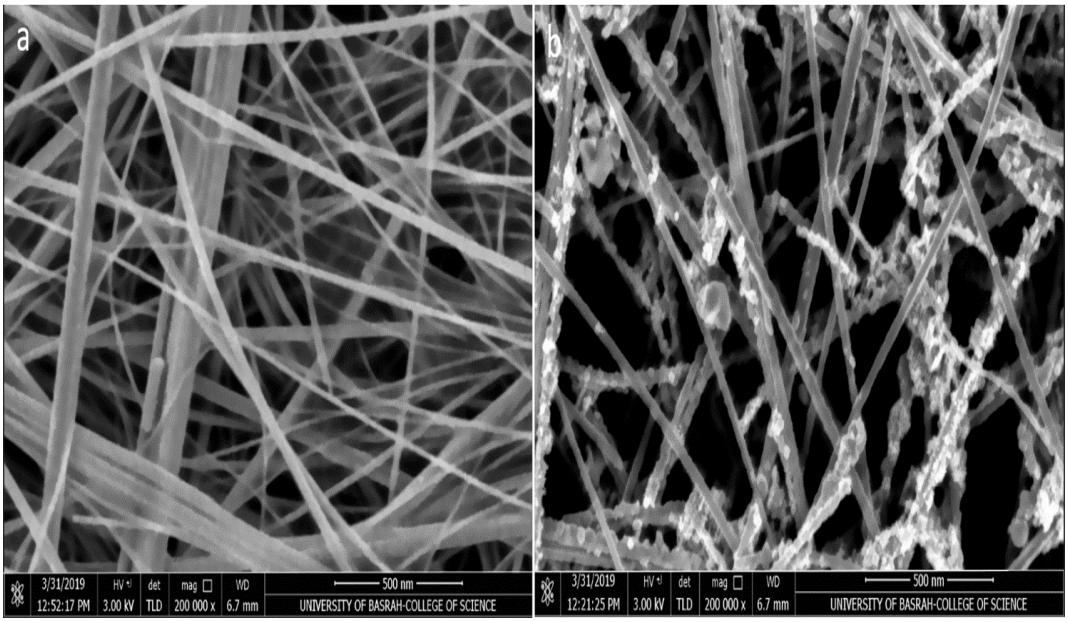

Figure 5-FESEM images of (a) AgNWs and (b) AgNW@AgNPs.

4- ***UV-visible absorption spectra***

Figure-6 illustrates the UV–visible absorption spectra of AgNPs with different concentrations (2×10^{-5}, 4×10^{-5}, 6×10^{-5}, 8×10^{-5}, 1×10^{-4} M); with and without R6G dye (1×10^{-6} M). Surface plasmon resonance peaks were distinctive and their locations were almost constant. In Figure-6a, the SPR of the AgNPs appeared at 404 nm and the SPR peak intensity was increased with increasing AgNPs concentration. The increase in the intensity of SPR peaks is due to the increase in the resonance between the collective oscillations of the conduction electrons with incident electromagnetic field [21].

On the other hand, as shown in Figure-6b, the absorption peak position of R6G (1×10^{-6} M) was at 525 nm. The absorption peak of the R6G dye was increased with increasing AgNPs concentration. The SPR peaks of the AgNPs were decreased after AgNPs had been mixed with the dye, because the energy is transferred from the nanoparticles to the dye [22, 23].

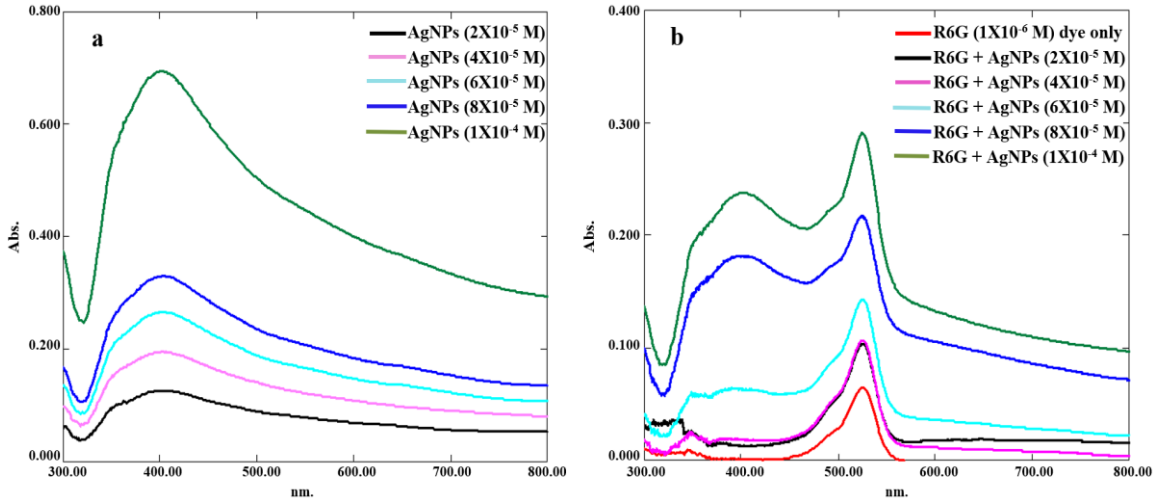

Figure 6-The UV–visible absorption spectra of different AgNPs concentrations (a) without R6G dye (b) with R6G dye (1×10^{-6} M).

Figure-7 illustrates the UV–visible absorption spectra of AgNWs at different concentrations (1×10^{-4}, 2×10^{-4}, 3×10^{-4}, 4×10^{-4}, 5×10^{-4}) with and without R6G dye (1×10^{-6} M). In Figure-7a, the SPR of the AgNWs has two peaks; the first appeared in 351 nm, due to the longitudinal plasmon resonance absorption of the AgNWs, and the second at 374 nm, due to the transverse plasmon resonance of AgNWs [24]. The intensity of these peaks was increased with increasing AgNWs concentration. On the other hand, as shown in Figure- 6b, the R6G dye molecules have an absorption peak at 524 nm and the intensity of this peak was increased with increasing AgNWs concentration. This behaviour can be illustrated as follows; Plasmonic metal nanostructures were shown to be able to enhance optical processes. The enhanced effect of surface absorption is enhanced based on the excitation of localized surface plasmons giving the enhanced electromagnetic fields. Thus, the molecules placed inside this enhanced field (which is adsorbed on the nanostructures) will be excited more often due to the electromagnetic field enhancement of the incident light on the active substrate, which leads to improve the absorption [22].

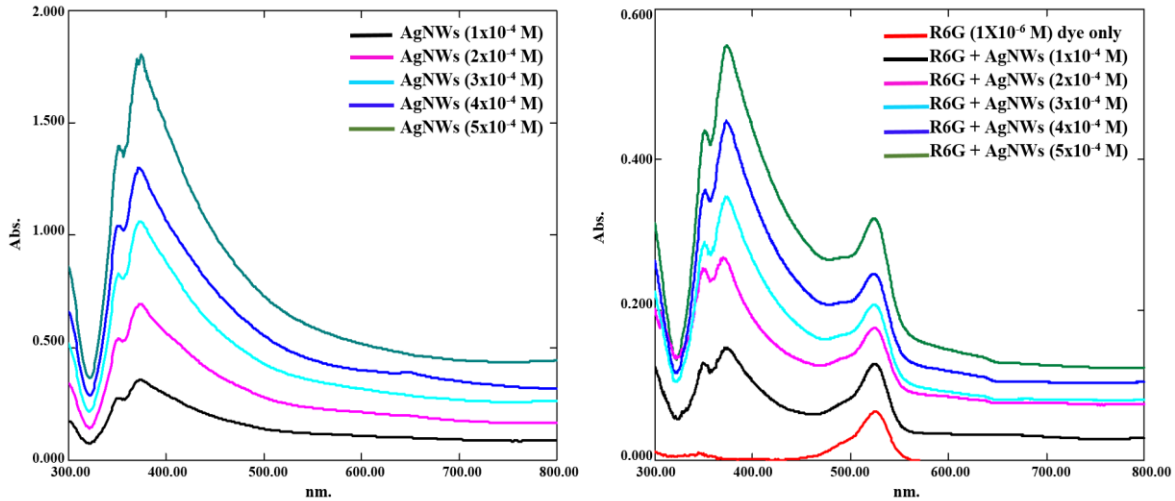

Figure 7- UV–visible absorption spectra of different AgNWs concentrations (a) without R6G dye (b) with R6G dye (1×10^{-6} M).

Figure-8 illustrates that two observed distinctive SPR peaks appeared at about 351 nm and 373 nm in the absorption spectrum of AgNWs. The peaks nearly vanished when the AgNWs were coated with PDA layer by self-polymerization, as seen clearly in the absorption spectrum of AgNW@PDA in Figure-8a. The absorption peaks of AgNW@AgNPs and AgNW@PDA@AgNPs were clearly observed at 391 nm and 400 nm, respectively. They have wider and higher absorption peaks, indicating the formation of plentiful AgNPs on the surfaces of the AgNWs and the PDA layer. The enhancement of the electromagnetic field arises due to the coupling between the LSP of AgNWs and the dense hot spots of the AgNW@AgNPs that were formed by the decoration of AgNPs on the surface of AgNWs. While the nanostructures were constructed by AgNPs-decorated AgNW@PDA to form AgNW@PDA@AgNPs nanostructures that have nanogaps between AgNWs and AgNPs that have surface plasmon polariton (SPP). The electromagnetic field was enhanced remarkably due to the coupling of LSP-LSP and LSP-SPP [25]. Moreover, the closely adjacent AgNPs usually exhibited a collective LSP mode, whose electromagnetic field was much stronger than that of the non-adjacent AgNPs. Therefore, AgNW@AgNPs and AgNW@PDA@AgNPs nanostructures can absorb more energy in the UV-visible range. The intensity of the electromagnetic field was increased with decreasing the distance between nanoparticles. This phenomenon needs more research.

Two peaks of the AgNWs (at 351 and 373) became less obvious due to the overlap of the two absorption peaks with the absorption peak of the AgNPs after forming the nanostructures. An absorption peak of the nanostructures became wider when they were mixed with the R6G dye. As clearly seen in Figure- 8b, the R6G dye molecules have absorption peaks at 524 nm and the intensity of this peak increased when R6G dye was mixed with AgNPs, AgNWs, AgNW@AgNPs and AgNW@PDA@AgNPs, with intensities of 0.237, 0.298, 1.1 and 1.128, respectively.

The SPR peaks of the AgNW@PDA@AgNPs nanostructures were enhanced more than those of the other nanostructures due to the notion that the SPR of metal nanostructures was largely sensitive to the dielectric environment around the surface morphology [26].

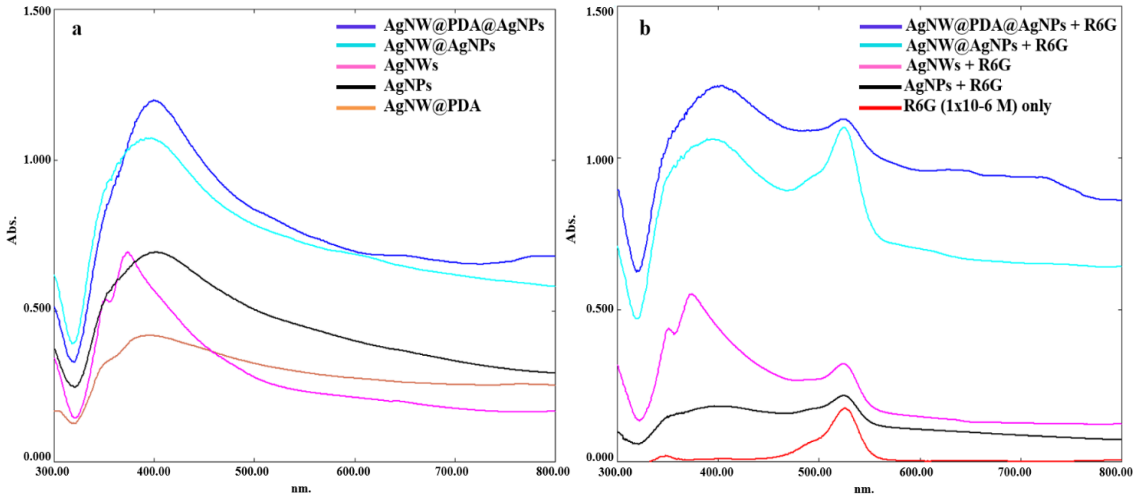

Figure 8- UV–visible absorption spectra of R6G dye and R6G with AgNPs, AgNWs, AgNW@AgNPs and AgNW@PDA@AgNPs nanostructures.

4- ***R6G dye Raman spectra***

Figure-9 shows the SERS spectra of R6G molecules for five nanostructures. The intensities of R6G peaks at 612, 775, 1186, 1312, 1361, 1510, 1577 and 1650 cm^{-1} were clearly observed. It was observed that the AgNW@AgNPs and AgNW@PDA@AgNPs nanostructures showed more remarkable Raman signal enhancement compared with AgNW@PDA, AgNPs, and AgNWs. For the AgNW@PDA nanostructures, the PDA layer weakened the SERS signal of R6G in a certain limit. The AgNW@PDA@AgNPs nanostructures have plentiful hot spots, interstices, and nanogaps (among AgNPs and AgNWs), which were synergistically subscribed to the strong SERS activity. Moreover, such small interstices among neighboring AgNPs and nanogaps between AgNWs and AgNPs in AgNW@PDA@AgNPs nanostructures were useful to achieve a very strong SERS signal [25].

To quantify the SERS enhancement factors (EFs) of R6G dye on the AgNW@AgNPs and AgNW@PDA@AgNPs substrates, the peak at 1650 cm^{-1} was used to calculate the SERS EFs using the following equation [27]:

$EF = (I_{SERS} / I_{bulk}) \times (C_{bulk} / C_{SERS})$

where I_{SERS} and I_{bulk} represent the intensities of the R6G dye, at a wave number of 1650 cm^{-1}, adsorbed to the nanostructures and those dissolved as bulk in solution, respectively. The C_{SERS} and C_{bulk} represent the concentrations of R6G dye utilized for the SERS experiments and the Raman, respectively. To calculate the enhancement factor (EF), the highest peak of the Raman signal was taken from the data of a directly practical drawing in Figure-9. As a result, the ISERS values at the wave number of 1650 cm^{-1}, that is a vibration mode (C–C stretching) for the AgNW@AgNPs and AsNW@PDA@AgNPs nanostructures exhibited by the SERS spectra in Figure-9, were equal to 46497.4 and 50508, respectively. Because the fluorescence is the dominant feature of the luminescence of aqueous drops of R6G dye, it is not possible to assign an appropriate value to the Raman signal (I_{bulk}). Thus, we suppose a maximum value of (I_{bulk}) in the range of the detector noise of 200 counts (A Raman spectrum of the R6G dye in deionized water with concentration of 1×10^{-1} M) [28,29]. The concentrations of R6G dye solution of 1×10^{-1} and 1×10^{-6} M were used for the (C_{bulk}) Raman without nanostructures and (C_{SERS}) experiments with nanostructures, respectively. As a result, the calculated EFs for the AgNW@AgNPs and AsNW@PDA@AgNPs nanostructures were 2.3×10^{7} and 2.5×10^{7}, respectively. The strong SERS signal enhancement of the electromagnetic field arises due to the coupling between the LSP of the AgNWs and the dense hot spots of the AgNW@AgNPs and AgNW@PDA@AgNPs nanostructures formed by the decoration of AgNPs on the surfaces of the AgNWs and AgNW@PDA. The AgNW@PDA@AgNPs nanostructure substrates have two types of coupling effect (LSP-LSP and control LSP-SPP) by PDA layer. For AgNW@AgNPs nanostructure, there exist the LSP-LSP coupling type and the non-controlled LSP-SPP coupling type [22, 25]. Table 1 illustrates the assignment vibration modes corresponding to the wave number and the enhancement factor (EF) of R6G (1×10^{-6} M) after being mixed with AgNW@PDA, AgNPs, AgNWs, AgNW@AgNPs and AgNW@PDA@AgNPs.

Table 1-The assignment vibration modes corresponding to wave number and the enhancement factor (EF) for Raman Spectra of R6G molecule.

Wave number (cm^{-1})	**Vibration mode**	**AgNW@ PDA**	**AgNPs**	**AgNWs**	**AgNW@ AgNPs**	**AgNW@PDA @AgNPs**
		EF	**EF**	**EF**	**EF**	**EF**
612	**C-C-C ring in-plane vibration**	**0.30×10^{7}**	**0.50×10^{7}**	**0.94×10^{7}**	**1.45×10^{7}**	**1.90×10^{7}**
775	**C-H out of-plane bend**	**0.24×10^{7}**	**0.59×10^{7}**	**0.75×10^{7}**	**1.20×10^{7}**	**1.40×10^{7}**
1186	**C-H in-plane bend**	**0.30×10^{7}**	**0.53×10^{7}**	**0.77×10^{7}**	**1.20×10^{7}**	**1.40×10^{7}**
1312	**N-H in-plane bend**	**0.26×10^{7}**	**0.46×10^{7}**	**0.80×10^{7}**	**1.30×10^{7}**	**1.50×10^{7}**
1361	**C-C stretching**	**0.27×10^{7}**	**0.74×10^{7}**	**1.06×10^{7}**	**2.17×10^{7}**	**2.42×10^{7}**
1510	**C-C stretching**	**0.41×10^{7}**	**0.66×10^{7}**	**1.00×10^{7}**	**2.03×10^{7}**	**2.23×10^{7}**
1577	**N-H in-plane bend**	**0.41×10^{7}**	**0.71×10^{7}**	**0.92×10^{7}**	**1.71×10^{7}**	**1.91×10^{7}**
1650	**C-C stretching**	**0.47×10^{7}**	**1.00×10^{7}**	**1.50×10^{7}**	**2.32×10^{7}**	**2.52×10^{7}**

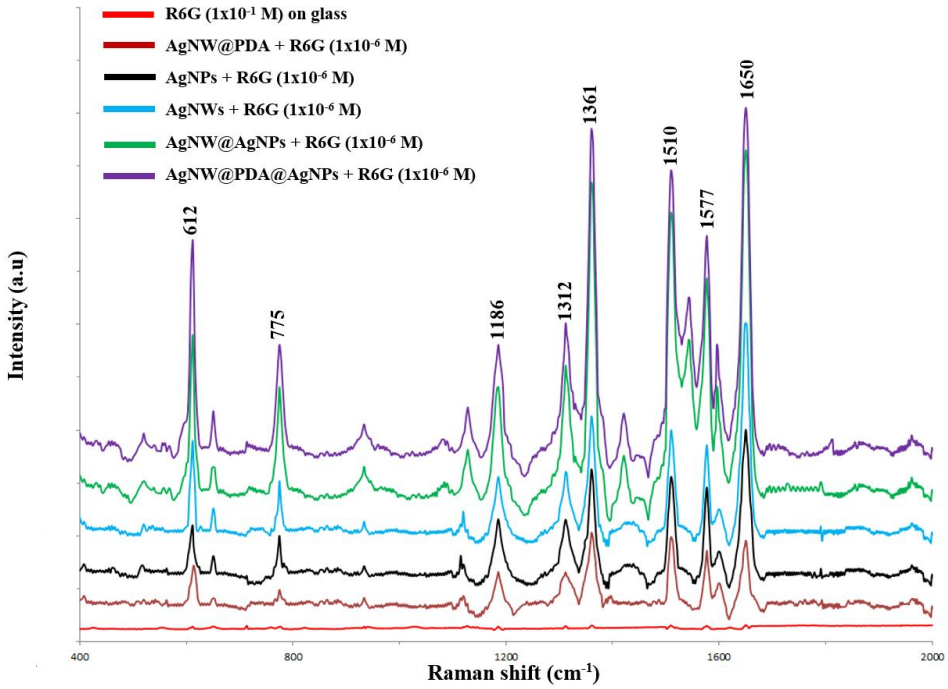

Figure 9-Raman spectra of R6G (1×10^{-1} M) on glass and R6G (1×10^{-6} M) mixed with AgNW@PDA, AgNPs, AgNWs, AgNW@AgNPs and AgNW@PDA@AgNPs substrates.

Conclusions

It can be concluded that EEW technique is a simple and efficient technique to fabricate nanostructures. The fabricated nanostructures can be used in the plasmonic substrates for Raman signal enhancement. The XRD patterns and the analysis of the images of FESTM and SETEM illustrated that the fabricated nanostructures have a rough surface and plentiful hot spots. The results indicated that the fabricated nanostructures have well absorption bands and excellent enhancement factor of R6G dye as probe molecules on the AgNW@AgNPs and AgNW@PDA@AgNPs nanostructures. It was verified that the AgNW@AgNPs and AgNW@PDA@AgNPs nanostructure substrates have the coupling effect of LSP-LSP and LSP-SPP, which was markedly related to the SERS enhancement of the R6G dye. Coupling of R6G dye molecules (as probe molecules) with fabricated nanostructures leads to the enhancement of many attractive optical and electronic properties utilized in a variety of applications such as chemical and biological sensors.

References

1. Hammad R. Humud and Saba J. Kadhem, **2015**. Laser-Induced Modification of Ag and Cu Metal Nanoparticles Formed by Exploding Wire Technique in Liquid. *Iraqi Journal of Science*, **56**(4B): 3135-3140.
2. Ahmed S. Wasfi, Hammad R. Humud, Noor K. Fadhil, **2019**. Synthesis of core-shell Fe3O4-Au nanoparticles by electrical exploding wire technique combined with laser pulse shooting. *Optics and Laser Technology*, **111**: 720–726.
3. Hammad R. Humud, **2016**. Effect of Ag nanoparticles on R6G laser dye hosted by PMMA polymerized by plasma jet. *Iraqi Journal of science*, **14**(29): 27-36.
4. J. Chen, Y. Huang, P. Kannan, L. Zhang, Z. Lin, J. Zhang, T. Chen and L. Guo, **2016**. Flexible and Adhesive SERS Active Tape for Rapid Detection of Pesticide Residues in Fruits and Vegetables. *Anal. Chem*, **88**(4): 2149–2155.
5. Yu Guo, Jing Yu, Chonghui Li, Zhen Li, Jiepan, Aihua Liu, Baoyuan Man, Tianfu Wu, Xianwu Xiu, and Chao Zhang, **2018**. SERS substrate based on the flexible hybrid of polydimethylsiloxane and silver colloid decorated with silver nanoparticles. *Optics Express*, **26**(17): 21784-21796.

6. G. Lu, H. Yuan, L. Su, B. Kenens, Y. Fujita, M. Chamtouri, M. Pszona, E. Fron, J. Waluk, J. Hofkens and H. Uji-i, **2017**. Plasmon-Mediated Surface Engineering of Silver Nanowires for Surface-Enhanced Raman Scattering. *J. Phys. Chem. Lett.*, **8**(13): 2774–2779.

7. H. Wei, F. Hao, Y. Huang, W. Wang, P. Nordlander and H. Xu, **2008**. Polarization Dependence of Surface-Enhanced Raman Scattering in Gold Nanoparticle−Nanowire Systems. *Nano Lett.*, **8**(8): 2497–2502.

8. Yi, Zao, Yi, Yong, Luo, Jiangshan, Ye, Xin, Wu, Pinghui, Ji, Xiaochun, Jiang, Xiaodong, Yi, Yougen, Tang, Yongjian, **2015**. Experimental and simulative study on surface enhanced Raman scattering of rhodamine 6G adsorbed on big bulk-nanocrystalline metal substrates. *RSC Advances*, **5**(3): 1718-1729.

9. S. Gwo, H.-Y. Chen, M.-H. Lin, L. Sun and X. Li, **2016**. Nanomanipulation and controlled self-assembly of metal nanoparticles and nanocrystals for plasmonics. *Chem. Soc. Rev.*, **45**(20): 5672–5716.

10. C.-nY. Li, M. Meng, S.-C. Huang, L. Li, S.-R. Huang, S. Chen, L.-Y. Meng, R. Panneerselvam, S.-J. Zhang, B. Ren, Z.-L. Yang, J.-F. Li and Z.-Q. Tian, **2015**. "Smart" Ag nanostructures for plasmon-enhanced spectroscopies. *J. Am. Chem. Soc.*, **137**(43): 13784–13787.

11. Z. Li, M. Wang, Y. Jiao, A. Liu, S. Wang, C. Zhang, C. Yang, Y. Xu, C. Li and B. Man, **2018**. Different number of silver nanoparticles layers for surface enhanced raman spectroscopy analysis. *Sens. Actuators B: chemical*, **255**: 374–383.

12. X. D. Tian, Y. Lin, J. C. Dong, Y. J. Zhang, S. R. Wu, S. Y. Liu, Y. Zhang, J. F. Li and Z. Q. Tian, **2017**. Synthesis of Ag Nanorods with Highly Tunable Plasmonics toward Optimal Surface-Enhanced Raman Scattering Substrates Self-Assembled at Interfaces. *Adv. Opt. Mater.*, **5**(21): 1700581.

13. S. J. Lee, A. R. Morrill and M. Moskovits, **2006**. Hot spots in silver nanowire bundles for surface-enhanced Raman spectroscopy. *J. Am. Chem. Soc*. **128**(7): 2200–2201.

14. C. Wang, B. Liu and X. Dou, **2016**. Silver nanotriangles-loaded filter paper for ultrasensitive SERS detection application benefited by interspacing of sharp edges. *Sens. Actuators B*: *chemical*, **231**: 357–364.

15. Seung Joon Lee, Jeong Min Baik, and Martin Moskovits, **2008**. Polarization-Dependent Surface-Enhanced Raman Scattering from a Silver-Nanoparticle-Decorated Single Silver Nanowire. *Nano Letters*, **8**(10): 3244-3247.

16. Alwan A. M., Mohammed M. S., & Shehab R. M., **2020**. The Performance of Plasmonic Gold and Silver Nanoparticle-Based SERS Sensors. *Iraqi Journal of Science*, **61**(6): 1320-1327.

17. H. Lee, S. M. Dellatore, W. M. Miller and P. B. Messersmith, **2007**. Mussel-Inspired Surface Chemistry for Multifunctional Coatings. *Science*, **318**(5849): 426–430.

18. Y. Liu, K. Ai and L. Lu, **2014**. Polydopamine and Its Derivative Materials: Synthesis and Promising Applications in Energy, Environmental, and Biomedical Fields. *Chem. Rev*., **114**(9): 5057–5115.

19. Ho, F.H.; Wu, Y.-H.; Ujihara, M.; Imae, T., **2012**. A solution-based nano-plasmonic sensing technique by using gold nanorods. *Analyst*, **137**(11): 2545–2548.

20. Roberto Pilot, Raffaella Signorini, Christian Durante, Laura Orian, Manjari Bhamidipati and Laura Fabris, **2019**. A Review on Surface-Enhanced Raman Scattering. *Biosensors*, **9**(2): 57.

21. Jayasmita Jana, Mainak Ganguly and Tarasankar Pal, **2016**. Enlightening surface plasmon resonance effect of metal nanoparticles for practical spectroscopic application. *RSC Adv*., **6**(89): 86174-86211.

22. Barzan, Mohammad, Hajiesmaeilbaigi, Fereshteh, **2016**. Effect of gold nanoparticles on the optical properties of Rhodamine 6G. *The European Physical Journal D*, **70**(5): 121.

23. S. F. Haddawi, Hammad R. Humud and S. M. Hamidi, **2020**. signature of plasmonic nanoparticles in multi-wavelength low power random lasing. *Optics and Laser Technology*, **121**: 105770.

24. M. B. Gebeyehu, T. F. Chala, S.-Y. Chang, C.-M. Wu and J.-Y. Lee, **2017**. Synthesis and highly effective purification of silver nanowires to enhance transmittance at low sheet resistance with simple polyol and scalable selective precipitation method. *RSC Adv*. **7**(26): 16139–16148.

25. Q. Ma, G. Liu, S. Feng, Y. Chen, a and W. Caib, **2018**. Interaction properties between different modes of localized and propagating surface Plasmons in a dimer nanoparticle array. *Optical Engineering*, 57(8): 087108.

26. Z. Zhang, T. Si, J. Liu, K. Han and G. Zhou, **2018**. Controllable synthesis of AgNWs@PDA@AgNPs core–shell nanocobs based on a mussel-inspired polydopamine for highly sensitive SERS detection. *RSC Adv*., **8**(48): 27349-27358.

27. Chunfang Wu, Enzi Chen, Jie Wei, **2016**. Surface enhanced Raman spectroscopy of Rhodamine 6G onagglomerates of different-sized silver truncated nanotriangles. *Colloids and Surfaces A: Physicochemical and Engineering Aspects*, **506**: 450-456.

28. S. Gupta, M. Agrawal, M. Conrad, N. A. Hutter, P. Olk, F. Simon, L. M. Eng, M. Stamm and R. Jordan, **2010**. Poly (2- (dimethylamino) ethyl methacrylate) Brushes with Incorporated Nanoparticles as a SERS Active Sensing Layer. *Adv. Funct. Mater*., **20**(11): 1756–1761.

29. Tzounis, Lazaros, Contreras-Caceres, Rafael, Schellkopf, Leonard, Jehnichen, Dieter, Fischer, Dieter, Cai, Chengzhi, Uhlmann, Petra, Stamm, Manfred, **2014**. Controlled growth of Ag nanoparticles decorated onto the surface of SiO2 spheres: a nanohybrid system with combined SERS and catalytic properties. *RSC Adv*., **4**(34): 17846-17855.